Expression of Tubb3, a Beta-Tubulin Isotype, Is Regulated by Androgens in Mouse and Rat Sertoli Cells 1

Authors: De Gendt, Karel, Denolet, Evi, Willems, Ariane, Daniels, Veerle W., Clinckemalie, Liesbeth, et al.

BioOne Complete (complete.BioOne.org) is a full-text database of 200 subscribed and open-access titles in the biological, ecological, and environmental sciences published by nonprofit societies, associations, museums, institutions, and presses.

BioOne sees sustainable scholarly publishing as an inherently collaborative enterprise connecting authors, nonprofit publishers, academic institutions, research libraries, and research funders in the common goal of maximizing access to critical research.

Expression of *Tubb3*, a Beta-Tubulin Isotype, Is Regulated by Androgens in Mouse and Rat Sertoli Cells[1]

Karel De Gendt,[3] Evi Denolet,[3] Ariane Willems,[3] Veerle W. Daniels,[3] Liesbeth Clinckemalie,[4]
Sarah Denayer,[4] Miles F. Wilkinson,[5] Frank Claessens,[4] Johannes V. Swinnen,[3] and Guido Verhoeven[2,3]

*Laboratories of Experimental Medicine and Endocrinology[3] and Molecular Endocrinology,[4] Catholic University
of Leuven, Leuven, Belgium*
Department of Reproductive Biology,[5] University of California in San Diego, La Jolla, California

ABSTRACT

Our previous analysis of Sertoli cell androgen receptor (AR) knockout (SCARKO) mice revealed that several cytoskeletal components are a potential target of androgen action. Here, we found that one of these components, the beta-tubulin isotype *Tubb3*, is differentially regulated in testes from SCARKO mice (relative to littermate controls) from Postnatal Day 10 to adulthood. The *Tubb3* gene is unique in this respect, as at Day 10, no other beta-tubulin genes are significantly regulated by AR. We further characterized androgen regulation of *Tubb3* in vivo and in vitro and demonstrated that it is a conserved feature in both mice and rats. To investigate whether androgens directly regulate *Tubb3* expression, we screened for androgen response elements (AREs) in the *Tubb3* gene. In silico analysis revealed the presence of four ARE motifs in *Tubb3* intron 1, two of which bind to AR in vitro. Mutation of one of these (ARE1) strongly reduced androgen-dependent reporter gene expression. These results, coupled with the finding that the AR binds to the *Tubb3* ARE region in vivo, suggest that *Tubb3* is a direct target of AR. Our data strengthen the contention that androgens exert their effects on spermatogenesis, in part, through modulation of the Sertoli cell cytoskeleton. Androgen regulation of beta-tubulin has also been described in neurons, fortifying the already known similarity in microtubule organization in Sertoli cell processes and neurons, the only other cell type in which *Tubb3* is known to be expressed.

androgen receptor, androgens, cytoskeleton, fertility, microtubules, testis

INTRODUCTION

The cellular and molecular mechanisms by which androgens control germ cell development remain incompletely understood. The majority of data indicate that adult germ cells do not express a functional androgen receptor (AR) and that androgens affect spermatogenesis indirectly via AR-expressing somatic cells such as Sertoli cells (SCs) or peritubular myoid cells [1]. Selective ablation of the AR in SCs causes a complete block in meiosis, supporting the contention that SCs play a key role in the control of spermatogenesis by androgens [2]. Interestingly, a comparable disturbance of spermatogenesis has recently been observed in mice with a selective ablation of the AR in peritubular cells [3]. Also in this model, however, the effects on spermatogenesis may be largely mediated by changes in SC function.

Earlier studies have demonstrated that mice with a selective ablation of the AR in SCs (SCARKO) may represent a powerful tool to unravel the molecular mechanisms by which androgens control spermatogenesis [2]. A search for genes that are differentially expressed in SCARKO and control testes at the onset of meiosis (Postnatal Day 10), revealed that—already at this early time point—the expression of 692 genes was significantly affected by the presence/absence of a functional AR in SCs [4]. For 40 of these genes the transcript levels in SCARKO and control mice differed by a factor of two or more. The validity of this approach for the identification of relevant androgen-regulated genes was supported by the observation that the shortlist of strongly regulated genes contained at least three genes that were previously shown to be essential for male fertility and six genes previously shown to be androgen regulated in the testis or in other organs [4].

One of the most intriguing genes in the shortlist of genes with markedly impaired expression in SCARKO testes is *Tubb3*. *Tubb3* (also known as Class III β-tubulin or *Tuj-1*) is a member of a family of genes that encode β-tubulin isotypes in vertebrates. Its expression is limited to the testis and to terminally differentiated neurons of the central and peripheral nervous system, where it is widely used as a marker for terminal neuronal differentiation [5–7]. TUBB3 has a characteristic "isotype-defining" carboxy-terminal motif (EESEAQGPK) that is highly conserved in chicken, mouse, rat and human [8, 9]. Beta-tubulins heterodimerize with α-tubulins to form microtubules, which are essential components of the cytoskeleton. As such, they play an important role in a variety of cellular functions, including determination of cell shape, trafficking of intracellular organelles, and mitosis [10]. Aberrant expression of *Tubb3* in tumor cells has been associated with increased resistance to microtubule-stabilizing chemotherapeutic agents such as paclitaxel [11], but the specific role of *Tubb3* in the testis is unknown.

Taking into account earlier data suggesting that tubular restructuring may be an important target of androgen action at the onset of meiosis and that the cytoskeleton is expected to play an important role in this process [4, 10, 12], we examined the effects of androgens on *Tubb3* expression in a variety of

experimental models. Evidence is presented that *Tubb3* mRNA and protein levels are controlled by androgens not only in mouse but also in rat testis and that *Tubb3* expression is specifically located in SCs. To distinguish between direct and indirect androgen regulation, we searched for potential androgen response elements (AREs) in the *Tubb3* gene and identified one potent ARE in the first intron.

MATERIALS AND METHODS

Animal Treatments

Animals were treated according to the National Institutes of Health Care and Use of Laboratory Animals and all experiments were approved by the local ethical committee.

SCARKO and control mice were bred by crossing male mice homozygously expressing AMH-Cre (C57BL/6SJL) with female mice (Ar^{fl/+}) carrying a mutated AR with a floxed second exon (98% CD1). Genotyping was performed as described previously [2].

The effect of testosterone propionate (TP) and of the antiandrogens bicalutamide and flutamide was studied in 7-day-old male C57BL/6J@Rj mice or Wistar rats (Janvier). Bicalutamide was kindly provided by AstraZeneca and flutamide and TP were purchased from Fluka and Sigma respectively. Stock solutions of these compounds were prepared in ethanol and further diluted in arachis oil. Mice received 50 µg animal^{-1} day^{-1} (50 µl arachis oil containing 10% ethanol) and rats 100 µg animal^{-1} day^{-1} (100 µl) of each of the mentioned compounds for 5 days sc. Treatment groups consisted of five animals, except for the control group in the mouse experiment, which consisted of three animals. At Day 12, mice and rats were killed and individual testes were snap frozen in liquid nitrogen and weighed before RNA preparation. Urogenital systems were fixed in Bouin fluid and seminal vesicles were dissected and weighed after fixation.

Primary SC Cultures and Organotypic Testis Cultures

Primary cultures of SC were prepared from 19-day-old rat and mouse testes as described previously [13]. After 4 days of culture, cells were washed four times with PBS (Invitrogen) and treated as indicated. Organotypic cultures of prepubertal mouse testes were set up as described previously [14] and incubated for 48 h with Dulbecco modified Eagle medium (DMEM)/F12 medium (Invitrogen) supplemented with vehicle (ethanol), R1881 (Perkin Elmer), recombinant human follicle-stimulating hormone (rhFSH; Puregon, Organon), bicalutamide, ketoconazole (MP Biomedicals) or combinations of these agents as indicated.

Quantitative PCR

RNA was extracted with the RNeasy mini kit (Qiagen) according to the manufacturer's instructions, including an on-column DNaseI-treatment (Qiagen). For testicular tissue samples, 5 ng of luciferase mRNA (Promega) was added to the whole testis sample at the start of the RNA extraction procedure to control for the efficiency of RNA extraction, RNA degradation, and the reverse transcription step and to allow specific mRNA levels to be expressed per testis [15]. One microgram of total RNA was reverse transcribed with the Superscript II RNase H reverse transcription kit (Invitrogen) including RNaseOUT (Invitrogen), according to the manufacturer's instructions and using 150 ng random primers (Invitrogen) per reaction.

The 7500 Fast Real-time PCR system (Applied Biosystems) was used for sample cDNA quantification. *Tubb* isotypes, *luciferase*, *Rn18s* and *Rpl19* were assayed using SybrGreen as a fluorescent dye. The relevant primers were described previously [4, 15] or are presented in Table 1. The quantitative RT-PCR (qPCR) two-step protocol was 2 min at 50°C followed by 2 min at 95°C. Subsequently, 40 cycles of 3 sec at 95°C and 30 sec at 60°C were performed. Each 10-µl real-time PCR reaction contained 1× Platinum SybrGreen qPCR Supermix-UDG (Invitrogen), 1× ROX dye (Invitrogen), 150 nM of each primer, and 2 µl of a 1:10 dilution of the cDNA reaction (1:1000 dilution for *Rn18s*). Dissociation curves confirmed uniqueness of each amplicon.

To create standards for the qPCR, gene-specific cDNAs were generated by RT-PCR. The fragments were then cloned into pGEM-T Easy (Promega), sequenced to confirm their identity, and quantified by spectrophotometry. All samples and standard curves were run in triplicate. Data were analyzed with 7500 Fast System SDS Software, version 1.4 (Applied Biosystems). *Rn18s* rRNA or *Rpl19* mRNA was used as an internal control and expression levels were calculated as copy number per 10^8 copies *Rn18s* rRNA or per 10^3 copies

Rpl19 mRNA. For testicular tissue samples, expression levels were calculated as copy number per 10^8 copies *luciferase* mRNA.

Western Blotting

Testes were homogenized with a Dounce homogenizer in 1× sample buffer (Invitrogen) containing β-mercaptoethanol. For cells, dishes were washed once in PBS, cells were scraped in 1× sample buffer, and the homogenate was passed 10 times through an 18G needle. Protein concentration was determined using a bicinchoninic acid procedure (Pierce Biochemical Company). Twenty micrograms of protein was separated on a NuPAGE 3%–8% Tris-Acetate gel (Invitrogen) and blotted onto a Hybond ECL nitrocellulose membrane (GE Healthcare). Membranes were blocked in 2% casein in TBS-T (25 mM Tris-HCL, 0.9% NaCl, 0.1% Tween, pH 7.4) and were incubated overnight with antibodies against TUBB3 (SDL.3D10, 1:5000, Sigma), TUBB5 (SAP.4G5, 1:20 000, Sigma), TUBB2C (7B9, 1:1000, Sigma), TUBB2A and TUBB2B (ONS.1A6, 1:400, Sigma), general β-tubulin (tub 2.1; 1:2000, Sigma), or β-actin (1:10 000; Cell Signaling Technology) in 5% nonfat dry milk in TBS-T. Immunoreactive signals were detected by incubation with Mouse TrueBlot ULTRA horseradish peroxidase-conjugated anti-mouse IgG (eBioscience Ltd.) followed by chemiluminescent detection using the Western Lightning Chemiluminescence Reagent Plus Kit (Perkin Elmer). The monoclonal antibodies used are specifically directed against a synthetic peptide representing the isotype-defining carboxyterminal amino acid sequence of β-tubulins [16–18]. Given that the ONS.1A6 antibody is raised against C-terminal peptide that is common to TUBB2C and TUBB4, it theoretically recognizes both proteins [16]. However, it was shown previously that TUBB4 is not expressed in the testis [19].

Immunohistochemistry

Mice (control and SCARKO at Days 10 and 140) and adult rats were killed and testes were fixed in Bouin solution for 6 h at room temperature. Tissues were processed into paraffin using standard techniques and sectioned at 5-µm thickness. Beta-tubulin proteins were detected by immunohistochemistry using standard methods described in detail previously [20]. Briefly, antigen retrieval in 0.01 M citrate buffer, pH 6.0, was performed, followed by endogenous peroxidase activity blocking by incubation of slides in 3% (vol/vol) H_2O_2 in methanol. Slides were incubated overnight at 4°C with primary antibody against TUBB3 (T2200, 1:20 000 dilution for mouse; SDL.3D10, 1:10 000 dilution for rat; Sigma), TUBB5 (SAP.4G5, 1:100 000, Sigma), TUBB2C (7B9, 1:100, Sigma), TUBB2A and TUBB2B (ONS.1A6, 1:300, Sigma), and general β-tubulin (tub 2.1; 1:500, Sigma). Slides were then incubated with biotinylated goat-anti-rabbit or rabbit-anti-mouse secondary antibody (DAKO) followed by incubation with streptavidin-conjugated horseradish peroxidase (DAKO) and visualization of immunostaining using diaminobenzidine (Liquid DAB+; DAKO). To ensure reproducibility of results and accurate comparison of immunostaining between treatment groups, sections from different genotypes were run in parallel on at least three occasions. Representative sections were photographed using a Leica DMR microscope (Leica) fitted with a Sony DXC 9100P 3CCD color video camera (Sony) and captured with Leica LIDA software version 1.60 (Leica Microsystems Imaging Solutions Ltd.). Images were compiled using Coreldraw 9 (Corel Corporation).

Plasmids

All genomic *Tubb3* fragments tested were derived from the BAC clone RP23-34O22 (obtained from CHORI, http://bacpac.chori.org/home.htm). Fragments were isolated either by restriction digestion or by PCR amplification (for primers see Table 1). Luciferase reporter plasmids were constructed using the pGEM-4Z as a basic vector. A minimal promoter containing the human E1b TATA box [21] was inserted in this vector in front of the luciferase reporter gene from the pGL4 vector (Promega) [22]. All PCR fragments were cloned into the basic reporter vector using the *NheI* restriction site. For DNA fragments obtained by restriction digestion, fragments and linearized vector were blunted before ligation. Mutations were introduced using the QuickChange II site-directed mutagenesis kit (Stratagene) with appropriate primers (Table 1).

Transfection Experiments

COS-7 (American Type Culture Collection) and SK11 cells (obtained from Dr. P. Saunders, Edinburgh, U.K.) were plated in a 96-well plate at 10^5 and 5.10^4 cells/well respectively in DMEM glutamax medium (Invitrogen) supplemented with 10% fetal calf serum (Hyclone) and antibiotics. COS-7 cells were maintained at 37°C, and SK11 cells were grown at 34°C [23]. After 24 h, cells were transfected using GeneJuice transfection reagent (Novagen) in 96-well plates with 100 ng luciferase reporter vector, 10 ng of the hAR

TABLE 1. List of primers.

Primer name	Sequence[a]	Application/fragment
Tubb1-fw	GGATTCCCAACAATGTCAAGGT	QPCR mouse Tubb1
Tubb1-rev	CAGGAAGGTAGCTGCCATGTTC	QPCR mouse Tubb1
Tubb2a-fw	CCTCCACCCCTTCTACAACCA	QPCR mouse Tubb2a
Tubb2a-rev	CCAAAACTTAGCGCCGATCT	QPCR mouse Tubb2a
Tubb2b-fw	CGGTTCCGGAGTAAGTTCCA	QPCR mouse Tubb2b
Tubb2b-rev	GCATGGTGCCTGGTTAGCTT	QPCR mouse Tubb2b
Tubb2c-fw	GGGAGCAGTGTGAACTCTTTATTCA	QPCR mouse Tubb2c
Tubb2c-rev	AGGACACAGGACAGCAAATGC	QPCR mouse Tubb2c
Tubb4-fw	TCACTCTGGCTCCCGTAAGTC	QPCR mouse Tubb4
Tubb4-rev	AGCACTTCTCTGGTAGGAACTGAAC	QPCR mouse Tubb4
Tubb5-fw	GGGTGCGGCAAGGTCTT	QPCR mouse Tubb5
Tubb5-rev	AGACCCAGGTGGAAACATACTTTC	QPCR mouse Tubb5
Tubb6-fw	TGTCACTGGCCCCTCTCAA	QPCR mouse Tubb6
Tubb6-rev	CCTGGTCTGCTGGGACTGTT	QPCR mouse Tubb6
L19-fw	CTGAAGGTCAAAGGGAATGT	QPCR mouse *Rpl19*
L19-rev	GGACAGAGTCTTGATGATCTC	QPCR mouse *Rpl19*
T3-intron01	*TCTAGA*GCAACCAGATAGGGG	452 bp, 902 bp
T3-intron02	*GCTAGC*CTGTACATGCCTGGATCCC	488 bp, 1042 bp
T3-intron03	*TCTAGA*ACTGTCTAGTTCTCCAGTGG	452 bp
T3-intron04	*TCTAGA*GAGGTTGGGCTTCTGCAGG	902 bp
T3-intron04bis	*GCTAGC*GAGGTTGGGCTTCTGCAGG	488 bp
T3-intron05	*GCTAGC*GAGCAGATGTTCGTCCAGG	1042 bp
T3-intron06	*GCTAGC*CTCAAATACTGATCAGAAGAGG	1323 bp
T3-intron08	*GCTAGC*AACTCAGAAATCTGCCTGCC	965 bp, 222 bp, 545 bp
T3-intron09	*GCTAGC*AGCACTCAGGAGGTAGAGG	1323 bp
T3-intron10	*GCTAGC*GGTTCTACACAGCTCGAGG	965 bp, 156 bp
p965-1	ATGCGA*GCTAGC*TGTCAGCACAAGCCGATGCC	200 bp
p965-2	ATGCGA*GCTAGC*AGTCAGCAAGTGCCAGTCC	222 bp
p965-3	ATGCGA*GCTAGC*AGGGATCTCAGAGCCCAAGG	198 bp-a
p965-4	ATGCGA*GCTAGC*AGGGGGGCTGCCTCCTTGG	200 bp
p965-5	ATGCGA*GCTAGC*GAGCCTGTTGTCATGCAG	196 bp
p965-6	ATGCGA*GCTAGC*TGTTCCCACTCTGTACAATGG	545 bp, 198 bp-a, 101 bp
p965-7	ATGCGA*GCTAGC*GGGGCTGAGTGTAGCAGCC	198 bp-b
p965-8	ATGCGA*GCTAGC*GCAACACCCAGGATGGTTGG	196 bp
p965-9	ATGCGA*GCTAGC*CAAGATGGACTCTGTCAGAGG	156 bp
p965-10	ATGCGA*GCTAGC*AGAGCCTGGGCAAGTCATGG	198 bp-b
p965-11	*GCTAGC*CAGCCCTTTCATCCCCTCCC	101 bp
pTubb3mut.1	CCAGAAC<u>AGAAGG</u>CTG<u>T**T**TTCT</u>CACAAGAG	Site-directed mutagenesis
pTubb3mut.2	ACAACAGGCTCTTGTG<u>AGAA**A**A</u>CAG<u>CCTTC</u>	Site-directed mutagenesis
Luci seq	GAGTGGGTAGAATG	Sequencing
pGS-Tubb3AREfw	CTAGCCAT<u>AGAAGG</u>CTGT<u>GTTCT</u>CAAC	EMSA ARE1
pGS-Tubb3ARErev	TCGAGTTG<u>AGAACA</u>CAG<u>CCTTC</u>TATGG	EMSA ARE1
pGS-Tubb3AREfwmut	CTAGCCAT<u>AGAAGG</u>CTG<u>T**T**TTCT</u>CAAC	EMSA competition ARE1
pGS-Tubb3ARErevmut	TCGAGTTG<u>AGAA**A**A</u>CAG<u>CCTTC</u>TATGG	EMSA competition ARE1
pGS-ARE2-fw	CTAGCCAT<u>TAGTTTT</u>GG<u>TGTTCCC</u>CAAC	EMSA ARE2
pGS-ARE2-rev	TCGAGTTG<u>GGGAACACC</u>A<u>AAACTAA</u>TGG	EMSA ARE2
pGS-ARE3-fw	CTAGCCAT<u>TAGTCTGC</u>AT<u>GTCCTC</u>AAC	EMSA ARE3
pGS-ARE3-rev	TCGAGTTG<u>AGGACA</u>TGC<u>AGACTAA</u>TGG	EMSA ARE3
pGS-ARE4-fw	CTAGCCAT<u>AGAACG</u>CAAT<u>GCTCCC</u>AAC	EMSA ARE4
pGS-ARE4-rev	TCGAGTTG<u>GGGAGCA</u>TTG<u>CGTTCT</u>ATGG	EMSA ARE4
pGS-ARE4mut-fw	CTAGCCAT<u>AGAACG</u>CAAT**T**<u>CTCCC</u>AAC	EMSA competition ARE4
pGS-ARE4mut-rev	TCGAGTTG<u>GGGAG**A**A</u>TTG<u>CGTTCT</u>ATGG	EMSA competition ARE4
Tubb3ARE1fw	TGGCCCCCAGAACAGAAG	ChIP *Tubb3* ARE1
Tubb3ARE1rev	TGGTGTTCCCACTCTGTACAATG	ChIP *Tubb3* ARE1
Tubb3Ctrlfw	TCACCACCTCCCTTCGATTC	ChIP *Tubb3* Ctrl
Tubb3Ctrlrev	CACCATGTTCACAGCCAGCTT	ChIP *Tubb3* Ctrl
rTubb3fw	GCCAAGTTCTGGGAGGTCATC	QPCR rat *Tubb3*
rTubb3rev	CCGAGTCCCCACATAGTTG	QPCR rat *Tubb3*
rRHOX5fw	CCATGATATCAGCCGCTTAC	QPCR rat *Rhox5*
rRHOX5rev	CCATGCTGTTCTTCCGAGTCT	QPCR rat *Rhox5*

[a] Half-sites of AREs are underlined; mutations with respect to the wild-type sequence are shown in bold; and restriction sites are depicted in italics.

expression plasmid [24], and 5 ng of CMV-β-galactosidase plasmid (Stratagene) per well as a control for transfection efficiency. For each reporter construct, triplicate wells were treated for 24 h with 10 nM R1881 or vehicle, starting 24 h after transfection. After correction for transfection efficiency, induction factors were calculated as the ratios of the average value of the luciferase value of the hormone-stimulated samples vs. vehicle-treated samples. An empty luciferase reporter vector and a 4xTAT-GRE construct [25] were included as negative and positive control respectively. As a supplementary negative control, a mirror experiment was set up in which no hAR expression plasmid was cotransfected. None of the investigated constructs was able to stimulate expression of the luciferase reporter after addition of R1881 in the absence of AR.

Electrophoretic Mobility Shift Analysis

Band shift assays were performed essentially as described previously [26] using cellular extracts from COS-7 cells transiently transfected with the hAR expression plasmid [27]. Partially overlapping oligonucleotides containing the ARE motifs or mutations thereof (Table 1) were radiolabeled with [α-^{32}P]dCTP
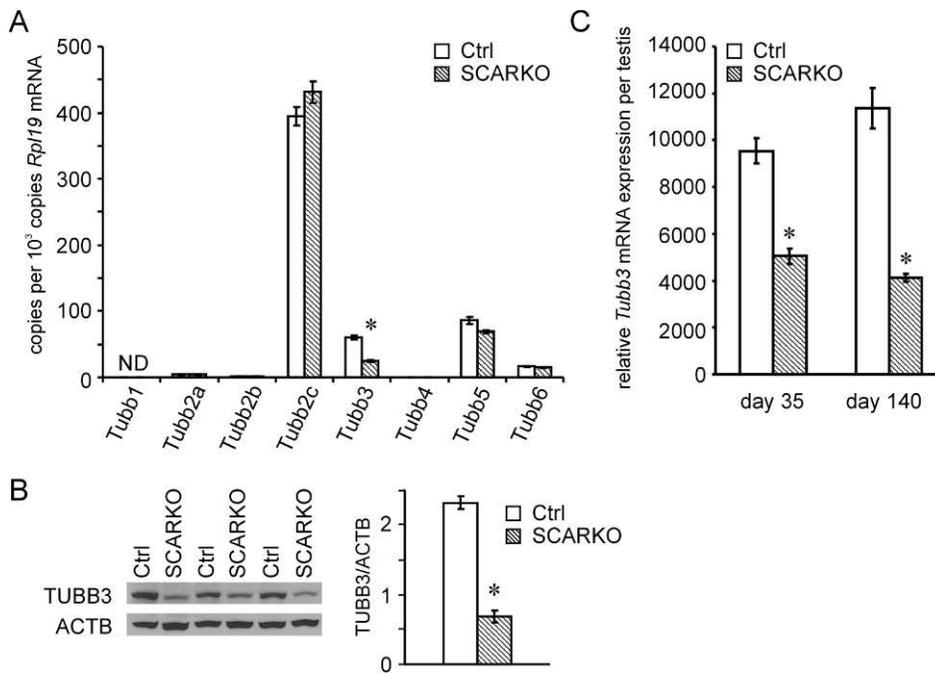
FIG. 1. Testicular expression of β-tubulin isotypes in SCARKO and control mice. **A**) The expression of different β-tubulin isotypes was assessed by qPCR. Expression levels were measured in control and SCARKO testes of 10-day-old animals. Data were normalized to *Rpl19* mRNA. Values represent the mean ± SEM of nine measurements. **B**) TUBB3 expression in 10-day-old control and SCARKO testes as determined by Western blotting (n = 6 per genotype). A representative Western blot is shown on the left. Beta-actin (ACTB) was used as a loading control. **C**) *Tubb3* mRNA expression in pubertal and adult (Day 35 and Day 140) testes of control and SCARKO mice as measured by qPCR. Data were normalized to a standard of exogenously added *luciferase* mRNA. Values represent the mean ± SEM of seven measurements. ND, not detectable; *P < 0.001 in comparison with the respective control group (AMHCre).

via a Klenow fill-in reaction. In-house anti-AR rabbit polyclonal antibody was added to the binding mixture to prove specific interaction between the AR and the probe. Competition experiments were performed with a 50- or 200-fold excess of unlabeled double-stranded oligonucleotide (wild-type ARE as the specific competitor; mutated ARE as the nonspecific competitor; Table 1).

Chromatin Immunoprecipitation

The detailed procedure for isolation of chromatin from adult mouse testes and the subsequent chromatin immunoprecipitation (ChIP) reaction is described in the Supplemental *Materials and Methods* (all Supplemental Data are available online at www.biolreprod.org). In short, immunocomplexes were pulled down after overnight incubation of the chromatin with anti-AR antibody (PG-21; Millipore) or rabbit IgG (negative control; Cell Signaling Technology). After washes, reverse cross-linking, and phenol-chloroform extraction of DNA, binding of AR to the *Tubb3* ARE region was determined by qPCR analysis. The presence of the *Tubb3* ARE region (primers were chosen to span ARE1; see Table 1) and a control region (*Tubb3* Ctrl; Table 1) in the samples was quantified with respect to the input. Recovered DNA in all samples was expressed as a percentage of the input, and the magnitude of recruitment for both genomic loci was calculated as the ratio of percentage of recovered DNA for the specific antibody sample over the percentage of recovered DNA for the nonspecific antibody sample.

Regulatory Sequences Analysis Tools

The Matrix-scan tool of the Regulatory Sequences Analysis Tools software package (http://rsat.ulb.ac.be/rsat/) [28] was used to screen for putative AREs using default settings and different thresholds for the *P* value as described earlier [22].

Statistical Analysis

Gene expression between different groups and treatments were compared by ANOVA followed by Fisher least significant difference (LSD) test using NCSS 2000 software (NCSS, Statistical Analysis and Data Analysis Software) unless indicated otherwise.

RESULTS

Tubb3, But Not Other Beta-Tubulins, Is Downregulated in SCARKO Testes

We previously identified *Tubb3* as an AR-regulated gene in the testis based on microarray analysis [4]. *Tubb3* transcript

levels were assessed by qPCR in testes derived from 10-day-old control and SCARKO mice, together with the transcripts encoding all other known β-tubulin isotypes. As shown in Figure 1A, the data confirm that ablation of the AR significantly decreases the expression levels of *Tubb3* mRNA (by 60%), whereas expression of other β-tubulin isotypes is not significantly affected. The data also demonstrate that *Tubb3* is one of the most prominent β-tubulin isotypes in the testis at this age. The reduction in *Tubb3* mRNA level is paralleled by a comparable reduction (down to 30%) in TUBB3 protein level (Fig. 1B). Quantitative RT-PCR measurements on Days 35 and 140 were performed to verify whether the reduction in *Tubb3* expression persists throughout puberty and adulthood (Fig. 1C). As the cellular composition of SCARKO and control testes differs significantly after d10, an external standard (luciferase mRNA) was added to the samples to allow normalization of *Tubb3* mRNA levels per testis. Figure 1C shows that *Tubb3* mRNA levels per testis remain significantly lower in d35 and d140 SCARKO testes than in control testes.

Antiandrogens Suppress Tubb3 Gene Expression in Wild-Type Prepubertal Mice and Rats

To confirm androgen regulation of *Tubb3* expression in an independent experimental paradigm, 7-day-old wild-type mice were treated for 5 days either with the antiandrogens flutamide or bicalutamide or with TP. *Rhox5* expression levels were measured as a positive control. Antiandrogen administration markedly decreased and TP administration increased seminal vesicle weight confirming the efficacy of treatment (Supplemental Table S1). Bicalutamide decreased *Rhox5* and *Tubb3* mRNA levels to 4.7% and 31.1% of those observed in vehicle-treated controls, respectively (Fig. 2, left panel). Flutamide caused a similar decrease in transcript levels (to 9.6% and 40.3% respectively).

Unexpectedly, TP also significantly reduced the expression of *Tubb3* (to 38.1%) and of *Rhox5* (to 54.3%). A plausible explanation for the reduction in expression in these AR-dependent genes, as well as for the 22% reduction in the relative testis weight after TP administration, is that already at
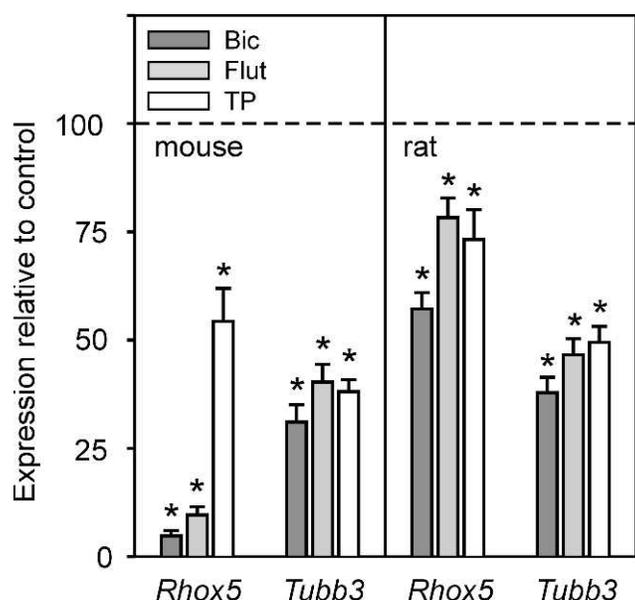
FIG. 2.   Antiandrogen and androgen treatment reduce *Rhox5* and *Tubb3* expression in prepubertal mice and rats. Quantitative RT-PCR analysis of testes from 12-day-old mice and rats treated for 5 days with bicalutamide (Bic), flutamide (Flut), testosterone proprionate (TP), or vehicle as described in *Materials and Methods*. Gene expression was normalized to *luciferase* mRNA added to the sample as an external standard. Results are expressed as a percentage of the expression observed in the controls (arbitrarily assigned a value of 100; dashed line). Values shown are means ± SEM. *$P < 0.05$ in comparison with the respective control group.

this early age, androgen administration reduces intratesticular androgen levels through a negative feedback effect on luteinizing hormone (LH) and follicle-stimulating hormone (FSH) secretion (as demonstrated below for the rat).

To explore whether androgen regulation of *Tubb3* could also be confirmed in another species, a qPCR assay was developed for the rat homologues of *Rhox5* and *Tubb3* and 7-day-old rats were exposed to the above described treatment protocol with antiandrogens and TP. Efficacy of treatment was again confirmed by the observed changes in seminal vesicle weight (Supplemental Table S1). The effects of the studied treatments on rat *Rhox5* and *Tubb3* transcript levels were comparable to those observed in mice, although the antiandrogen-induced decrease in transcript levels was less pronounced, particularly for *Rhox5* (Fig. 2, right panel). The bicalutamide- and flutamide-induced decrease in transcript levels occurred despite an approximately 2-fold and 4-fold increase in serum LH levels (Supplemental Fig. S1), which may have counteracted the effects of the antiandrogens by raising the intratesticular level of androgens. As in mice, TP treatment also significantly decreased both *Rhox5* and *Tubb3* expression levels. The decrease in relative testicular weight (by 26%) together with the decrease in LH and FSH serum levels associated with TP treatment (Supplemental Table S1 and Supplemental Fig. S1) confirm that the hypothalamo-pituitary-gonadal axis is functional at this age, and, accordingly, that TP treatment may have suppressed intratesticular androgen levels.

To avoid the confounding secondary changes (e.g., in the secretion of gonadotropins) inherent to in vivo systems, we also studied the effects of androgens and antiandrogens on *Tubb3* expression in a recently developed organotypic culture system [14]. As shown in Figure 3A, bicalutamide treatment for 48 h significantly reduced *Tubb3* expression in testicular explants from 8-day-old mice. In contrast, incubation with the synthetic androgen R1881 did not result in transcript levels exceeding those observed in the vehicle treated control (or in 8-day-old mice testes) indicating that *Tubb3* is maximally stimulated by endogenous androgens, as demonstrated for other androgen-regulated genes [14]. However, a clear stimulatory effect of androgens on *Tubb3* expression in this system was demonstrated
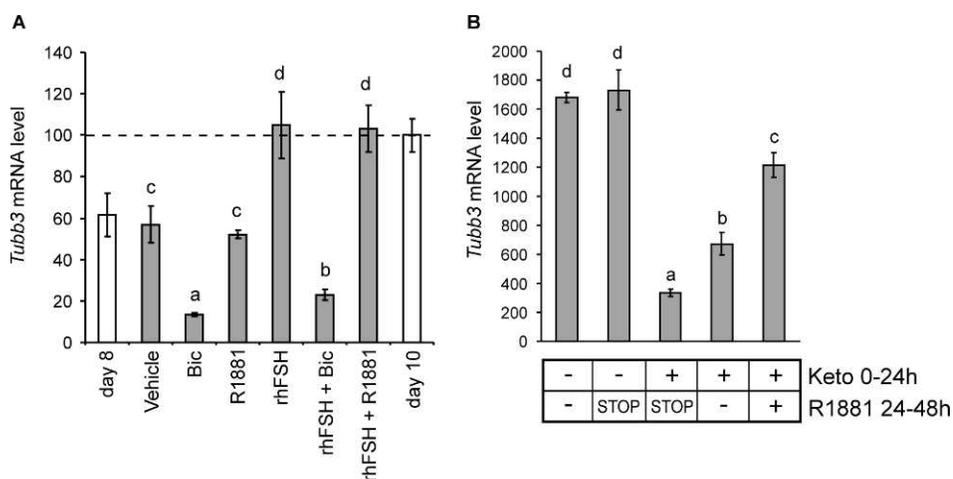

FIG. 3.   Hormonal control of *Tubb3* expression in organotypic cultures. **A**) Testicular explants from 8-day-old mice were cultured for 48 h in control medium (Vehicle) or in medium supplemented with R1881 (10^{-8} M), bicalutamide (Bic; 10^{-5} M), rhFSH (20 ng/ml) or combinations of these agents, as indicated. Expression levels of *Tubb3* were measured by qPCR (grey bars). As a control, expression levels were also measured in testis samples freshly derived from 8-day-old (day 8) and 10-day-old (day 10) mice processed in parallel (open bars). All measurements were normalized to the level of *Rn18s* and were expressed as a percentage of the values measured in testes from 10-day-old mice, arbitrarily set at 100 (dashed line). Values indicated are the mean ± SEM of five independent samples. **B**) Testicular explants from 8-day-old mice were pretreated for 24 h with control medium or with ketoconazole (Keto; 2.10^{-5} M) as indicated. Thereafter, incubations were either stopped (STOP) or continued after replacement of the medium by control medium or by medium supplemented with R1881 (10^{-8} M) and incubation was continued for another 24 h. Expression levels were determined using qPCR and are expressed relative to 10^8 copies of *Rn18s* as an internal control. The values are the mean ± SEM of four or five independent samples. ANOVA followed by Fisher LSD test was used to compare expression levels in cultured explants after log transformation. Values derived from freshly prepared Day 8 and Day 10 testes were not included in the statistical analysis. Values that differ significantly between each other ($P < 0.05$) are indicated by different letters (a, b, c, and d).
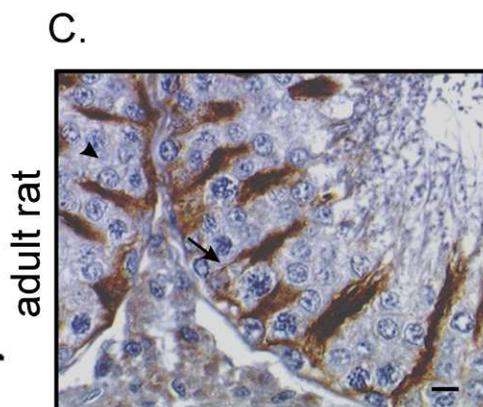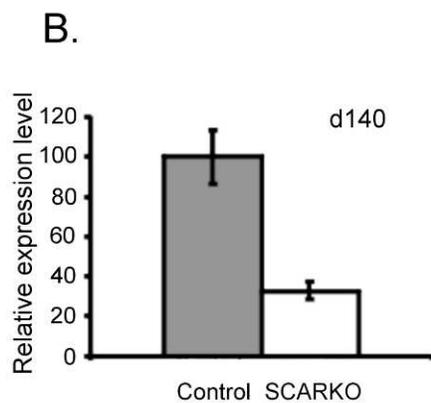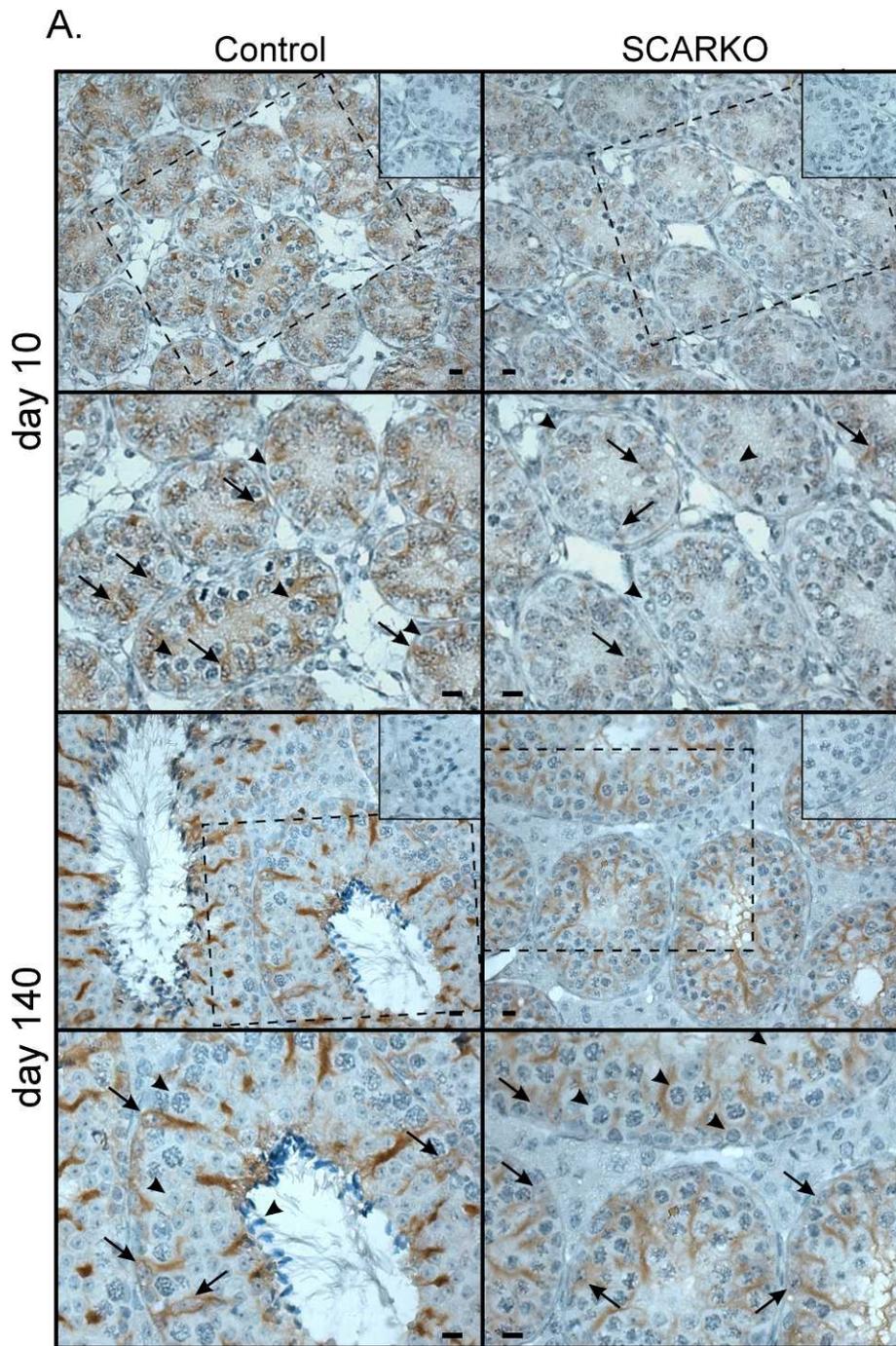
FIG. 4. Expression of TUBB3 protein in mouse and rat testes. **A**) Top row: immunostaining of TUBB3 (brown) in day 10 control (left) and SCARKO (right) mouse testes. Dashed rectangle: area selected for magnification in second row. Second row: high-power magnification of pictures in the top row for identification of cell types. Third row: immunostaining of TUBB3 in day 140 control (left) and SCARKO (right) mouse testes. Dashed rectangle: area selected for magnification in bottom row. Bottom row: high-power magnification of pictures in third row for identification of cell types. Insets: negative control. Arrows, SCs; arrowheads, germ cells. Bar = 10 μm. **B**) TUBB3 expression in 140-day-old control and SCARKO testes as determined by Western blot analysis. Densitometric quantification demonstrated decreased TUBB3 expression in SCARKO testes relative to control testes (n = 3 per genotype). **C**) Immunostaining of TUBB3 in adult rat testis. Arrows, SCs; arrowheads, germ cells. Bar = 10 μm.

upon treatment with R1881 after inhibition of endogenous androgen production by ketoconazole for 24 h (Fig. 3B). Interestingly, experiments with rhFSH revealed a dual mechanism of action for this hormone. First, rhFSH alone stimulated *Tubb3* mRNA level (without increasing testosterone production in the explants [14]); the level rose to that in 10-day-old mice testes (Fig. 3A). This effect was largely counteracted by bicalutamide, suggesting that rhFSH mainly acts through AR-dependent signaling to regulate *Tubb3* expression in SCs. Second, FSH increased *Tubb3* expression in explants derived from SCARKO mice (data not shown), indicating that FSH can stimulate *Tubb3* expression independently of AR. Further supporting this concept was the finding that explants cotreated with rhFSH and bicalutamide had significantly higher *Tubb3* expression than those treated with bicalutamide alone (Fig. 3A). In conclusion, our data indicate that androgens and FSH cooperate to control *Tubb3* transcription.

TUBB3 Protein Is Specifically Expressed in SCs in an AR-Dependent Manner

TUBB3 immunohistochemical staining of control and SCARKO testes of 10-day-old mice revealed intensive staining around SC nuclei with radial extensions to the base and center of the tubules. No staining was observed in developing germ cells, interstitial cells, or peritubular myoid cells (Fig. 4A, second row). Concordant with these data, staining was more intense in control than in SCARKO SCs (Fig. 4A, top row).

In testes from 140-day-old control mice, TUBB3 staining was also clearly confined to SCs. Staining was in a dense, spoke-like pattern radiating from the base of the seminiferous epithelium to the lumen. Bundles of TUBB3 staining touched the periphery of the tubules and clearly surrounded SC nuclei; extensive branching of stained bundles was seen around elongating spermatid heads. No staining was observed in interstitial cells, peritubular myoid cells, developing germ cells, or released spermatozoa (Fig. 4A, bottom row). Day 140 SCARKO testes also had SC staining but, as expected, the signal was weaker than in control testes (Fig. 4A, third row). The pattern of staining was also more variable. Some tubules show spoke-like structures comparable to those observed in control testes, whereas others displayed a more irregular honeycomb pattern of staining. No obvious difference in TUBB3 expression levels was observed between the different stages of the seminiferous epithelial cycle. Western blotting analysis confirmed lower TUBB3 protein expression in SCARKO vs. control testes (Fig. 4B).

Staining of adult rat testis for TUBB3 revealed a pattern of preferential SC localization very similar to that observed in mice (Fig. 4C). In rats, however, some staining was also noticed in the interstitial compartment.

To explore whether other β-tubulin isotypes are also expressed in SCs, adult mouse testes were also stained using antisera directed against TUBB2A/2B, TUBB2C, and TUBB5. An antiserum recognizing all β-tubulins was included as a control. As shown in Supplemental Figure S2, selective SC staining was also noted for TUBB2A/2B and TUBB5, whereas germ cell staining was noted for TUBB2C. The expression of TUBB2A/2B, TUBB3, and TUBB5 in SCs was confirmed by Western blotting experiments on SCs isolated from 19-day-old mice. Purified rat SCs expressed the same profile of β-tubulin isotypes (Supplemental Fig. S2).

Tubb3 Intron 1 Has an ARE

To explore whether the *Tubb3* gene may be directly regulated by androgens, we performed a functional screen for

AREs in the region extending from −7028 to +101 bp relative to the *Tubb3* transcription initiation site. To this end, fragments of the promoter, varying from 655 up to 7128 bp, were cloned into a luciferase reporter plasmid (Supplemental Fig. S3, A and B) and transfected into either COS-7 or SK11 cells together with an hAR expression plasmid. In COS-7 cells, the presence of the promoter fragments caused a limited (∼8-fold) increase in luciferase activity when compared to empty reporter vector (Supplemental Fig. S3B), but no further increase was observed after stimulation with the synthetic androgen R1881 (Supplemental Fig. S3C). In SK11 cells, an SC-derived cell line, the presence of the promoter fragments caused a marked (∼55-fold) increase in the basal expression level. The highest levels were obtained with the 655-bp proximal promoter fragment, suggesting that this fragment contains regulatory elements enhancing basal transcription, particularly in SCs. As in COS-7 cells, however, none of the constructs tested was able to mediate a further increase in luciferase expression after addition of R1881 (Supplemental Fig. S3, B and C).

Because AREs have also been described in the first intron of some androgen-regulated genes [29–31], we next screened a 5262-bp BamHI-XhoI-fragment (+647 to +5808) spanning nearly the entire *Tubb3* intron 1 (Fig. 5A) for its ability to enhance luciferase expression in the presence of an activated AR. As shown in Figure 5B, transfection of the 5262-bp fragment in COS-7 cells resulted in a ∼24-fold induction of luciferase activity after stimulation with R1881. Examination of the activity of different subfragments within and upstream of the 5262-bp fragment revealed that the activity was situated in a 965-bp region at the 3′ end of the intron (+4958 to +5922; ∼22-fold stimulation). Similar results were obtained in transfected SK11 cells, although the magnitudes of induction for the 5262-bp and the 965-bp fragments were slightly lower (∼8.0-fold and ∼10-fold respectively).

The 965-bp fragment was screened for consensus AREs using the matrix-scan tool of the Regulatory Sequences Analysis Tools software package [28]. With the P value threshold set at $\leq 10^{-4}$, one consensus-like ARE motif was identified, located at position +5439 to +5453 (AGAAGGctgTGTTCT; designated ARE1; $P = 9.2 \times 10^{-5}$). When the P value threshold was set at $\leq 10^{-3}$, three additional ARE motifs were identified, all located in the neighborhood of ARE1 at position +5497 to +5511 (TAGTTTtggTGTTCC; ARE2; $P = 6.5 \times 10^{-4}$), +5366 to +5380 (TAGTCT gcaTGTCCT; ARE3; $P = 8.1 \times 10^{-4}$) and +5588 to +5602 (AGAACGcaaTGCTCC; ARE4; $P = 1.0 \times 10^{-3}$).

To elucidate which, if any, of the predicted AREs mediated androgen responsiveness of the 965-bp fragment and to explore the possibility of other hidden nonconsensus AREs, we subcloned different overlapping parts of the 965-bp fragment in the reporter vector. In COS-7 cells, a prominent androgen response was observed with the 545-bp, 198-bp-a, and 101-bp fragments (92-, 184- and 38-fold stimulation, respectively). All these fragments contained the ARE1 sequence (Fig. 5C). Much lower degrees of stimulation (1.7- to 3.5-fold) were observed with fragments containing none, one, or more than one of the other predicted AREs (222 bp, 200 bp, 196 bp, 198 bp-b, and 156 bp). As with COS-7 cells, SK11 cells exhibited androgen induction with the 545-bp, the 198-bp-a, and the 101-bp fragments (11-, 9- and 3-fold induction, respectively). No consistent activity was observed with the other fragments investigated.

Taken together, these data suggest that ARE1 is the most active response element in the studied region. Interestingly, its activity seems to be enhanced by ARE3, as a reporter plasmid including both AREs (198 bp-a) showed a 4.9-fold (in COS-7
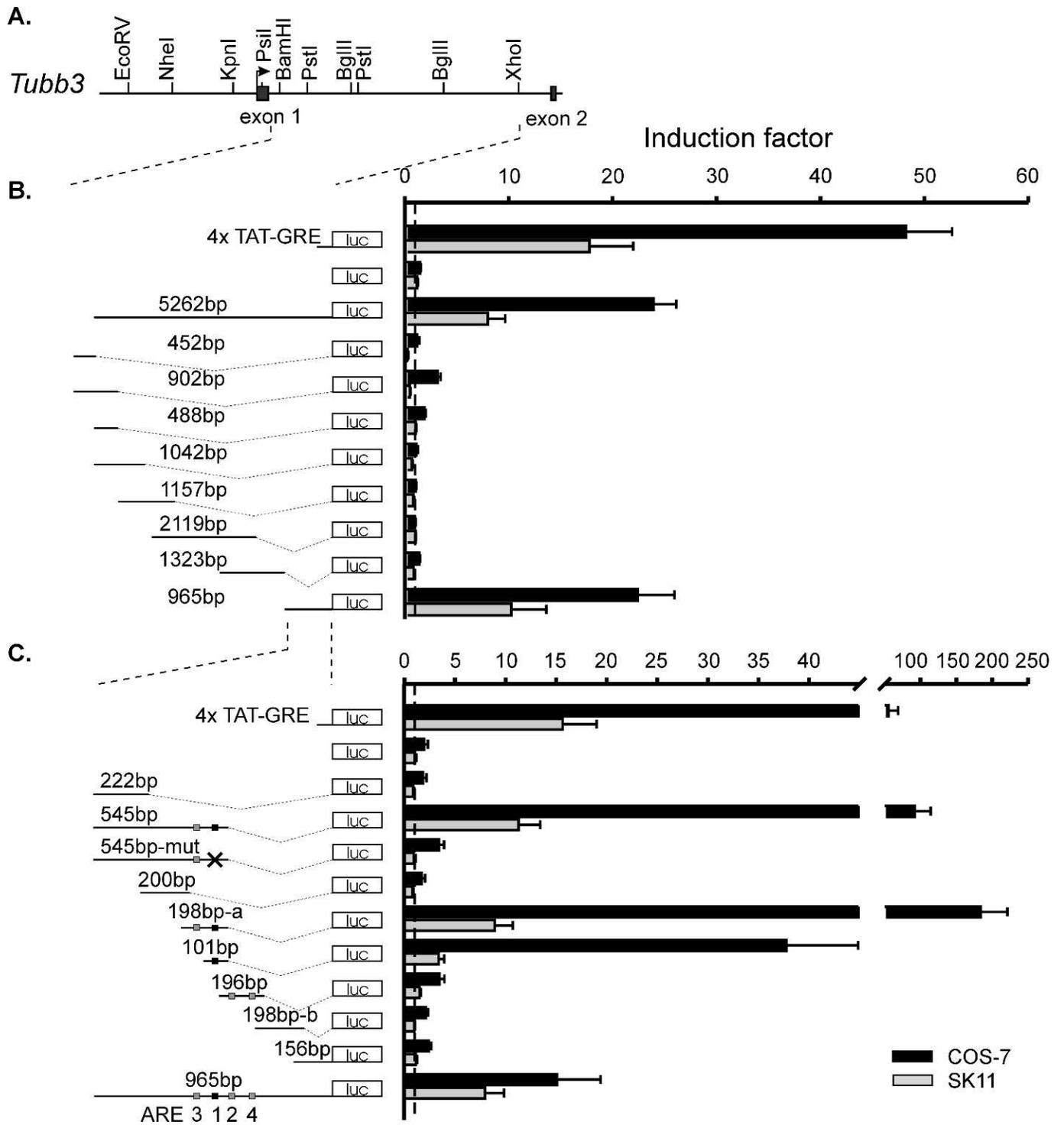
FIG. 5.   Identification of a functional ARE in the first intron of *Tubb3*. **A**) Restriction map of the *Tubb3* promoter and intron 1. Exons 1 and 2 are shown as rectangles. Arrow, start of transcription. **B**) Different fragments of *Tubb3* intron 1 were cloned into a luciferase reporter vector and tested for androgen responsiveness. In short, COS-7 and SK11 cells were treated 24 h after transfection with 10^{-8} M R1881 or vehicle for 24 h, as described in *Materials and Methods*. All results are presented as mean ± SEM of induction factors measured in four (COS-7) or five (SK11) independent experiments. A positive control (4xTAT-GRE) and a negative control (empty reporter vector) were included in each experiment. All fragments are identified by their length, as indicated. **C**) Subfragments of a 965-bp fragment were cloned into a luciferase reporter vector and tested for androgen responsiveness as described in **B**. Results are presented from six (COS-7) or five (SK11) independent experiments. Putative AREs are shown as squares, mutated ARE 1 is shown as a cross. Luc, luciferase reporter gene.
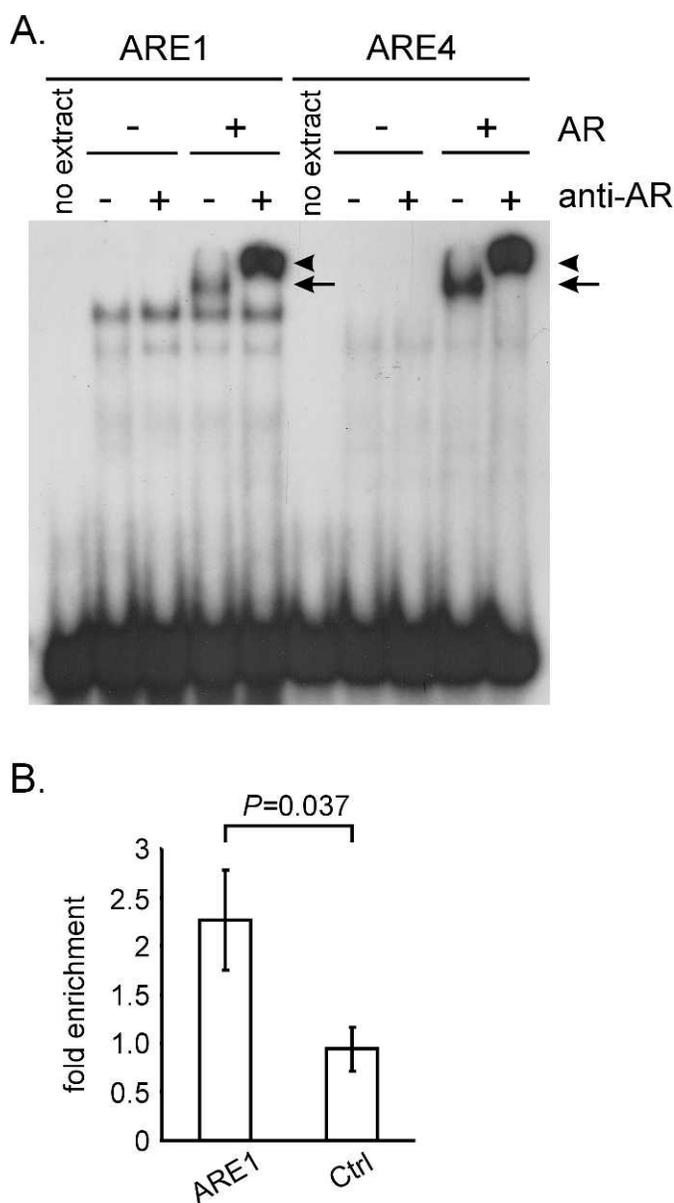
FIG. 6.   AR-*Tubb3* ARE Binding. **A**) EMSA using full-size AR constructs were performed with wild-type ARE1 and ARE4 radiolabeled probes, as described in *Materials and Methods*. Anti-AR antibody was added where indicated to demonstrate specificity of AR binding. Arrow, DNA-receptor complex; arrowhead, supershifted complex. **B**) ChIP analysis of adult mouse testes chromatin. Fold enrichment is expressed as the ratio of recovered DNA in the specific antibody sample over the nonspecific antibody sample (1-fold enrichment = no enrichment) as explained in *Materials and Methods*. Values are given as mean ± SEM for five independent experiments for the *Tubb3* ARE region (ARE1) and a negative control region located 4.2 kb upstream of the *Tubb3* ARE1 (Ctrl).

cells) and 2.3-fold (in SK11-cells) higher induction factor than a construct with ARE1 alone (101 bp). To definitively determine whether ARE1 promotes androgen responsiveness, we mutated the "**TG**TTCT" half-site of ARE1 to "**T**TTTCT" in the 545-bp fragment (545 bp-mut). This reduced androgen induction in COS-7 cells and SK11 cells by a factor of 27- and 12-fold respectively (Fig. 5).

Next, we investigated the ability of the identified AREs to interact with the AR in vitro using electrophoretic mobility shift analysis (EMSA). As shown in Figure 6A, addition of a cell extract containing AR clearly delayed the migration of a labeled probe containing ARE1 and ARE4. A supershift was observed in the presence of an AR antiserum for both AREs, confirming that the delay in migration was due to interaction with the AR. No binding was observed for ARE2 and ARE3 (Supplemental Fig. S4A). As evidence for specificity, competition experiments were performed in which a 50- and 200-fold excess of unlabeled WT and mutated ARE probes was added to the reaction (Supplemental Fig. S4B). Mutated ARE probes were designed to contain a 1-bp mutation that disrupts one half site of the ARE consensus sequence (see Table 1). For both AREs, a 50-fold excess of unlabeled WT probe was able to compete for binding of the AR to the labeled WT probe, an effect that was even more outspoken when a 200-fold excess unlabeled probe was applied. In contrast, competition with an unlabeled mutated probe (either 50-fold or 200-fold excess) did not affect binding of the AR to the labeled WT probe, demonstrating that the AR specifically binds to the ARE DNA sequence.

Finally, we performed ChIP assays on chromatin from adult testicular tissue with an antibody against AR to demonstrate in vivo binding of the AR to the *Tubb3* ARE region. Importantly, as the complete *Tubb3* ARE cluster spans only 237 bp, the resolution of the present ChIP experiment (with an average chromatin fragment size of 300 to 400 bp) does not permit identification of the specific ARE(s) bound, but rather allows determination of binding to the *Tubb3* ARE region as a whole. As demonstrated in Figure 6B, the *Tubb3* ARE region (ARE1) is significantly enriched 2.2-fold when ChIP is performed with a specific anti-AR antibody compared to a nonspecific antibody. In contrast, a control genomic region (Ctrl) situated 4.2 kb downstream of the *Tubb3* ARE1 is not enriched (factor 0.9). In conclusion, the data suggest that the AR binds specifically to the *Tubb3* ARE region in vivo.

DISCUSSION

Quantitatively normal spermatogenesis requires the action of both androgens and FSH [1]. Under a number of conditions, however, androgens are able to support complete germ cell development and fertility in the virtual absence of FSH [32–35]. Although androgens are sufficient to drive spermatogenesis, the molecular mechanisms by which they act remain poorly understood. Here we describe a new target for androgen action in the testis: *Tubb3*, a beta tubulin isotype that is uniquely expressed in SCs. Based on analysis of SCARKO mice, we show that AR activation promotes *Tubb3* mRNA and TUBB3 protein expression in testes from Postnatal Day 10 throughout adulthood. These early effects of androgens on *Tubb3* expression are also observed after treatment of prepubertal mice or organotypic cultures derived from prepubertal mouse testes with antiandrogens. Importantly, the ability of androgens to regulate *Tubb3* was a conserved response, as treatment of immature rats with androgens or antiandrogens also regulated *Tubb3* gene expression. Interestingly, *Tubb3* expression is also stimulated by FSH, thereby providing a potential point of interaction between these two important hormonal pathways that drive spermatogenesis.

Collectively, these results indicated that the effect of androgens on *Tubb3* is mediated by a pathway involving AR. To distinguish between the possibilities that the effect of androgens involves a direct interaction of the AR with the *Tubb3* gene or is indirectly mediated through an androgen-regulated intermediary transcription factor (as described for instance for the effects of androgens on genes involved in lipid metabolism [36]), we searched for functional AREs in the promoter region and in the first intron of the *Tubb3* gene. No

AREs were found in a fragment containing the first 7.1 kb of the 5′ upstream region of *Tubb3*. In contrast, several lines of evidence, including in silico analysis, transfection studies with reporter constructs, DNA-binding studies, and mutational analysis, revealed the presence of a potent ARE (ARE1) in the first intron of *Tubb3*. This ARE binds to AR in vitro and is crucial for androgen-dependent reporter expression, based on mutagenesis and transfection experiments. Further evidence for the functional importance of ARE1 is that ChIP experiments revealed that AR is recruited to the *Tubb3* ARE region in vivo. We also observed several other ARE-like motifs in the neighborhood of ARE1, but none shared with ARE1 the ability to both 1) bind AR in vitro and 2) stimulate reporter expression. However, this does not rule out that these other ARE-like motifs collaborate with ARE1 to drive AR-mediated transcriptional induction of *Tubb3*. Interestingly, a similar cluster-like organization of AREs has been observed to mediate direct androgen responsiveness of *Rhox5*, a strongly androgen-regulated gene in SCs [37, 38].

The finding of regulatory elements in the first intron of *Tubb3* is not completely unexpected, as a neuron-restrictive silencer element has also been located in the first intron of the chicken *Tubb3* gene (formerly known as *cβ4*) [39]. This element is conserved in mouse *Tubb3* intron 1. Moreover, the regulatory effect of the steroid hormone ecdysone on the expression of a β3-tubulin in *Drosophila* (expression of which is also confined to somatic cells in the gonad) is also mediated, at least in part, by sequences in the first intron of the corresponding gene [40]. Finally, several AREs in other genes have also been found to be located in intronic sequences [29–31].

The AR-induced changes in *Tubb3* expression observed here, together with an alteration in the expression of several other cytoskeletal genes [4, 10, 12, 41], suggest that the cytoskeleton is a target for androgen action in SCs. The microtubular system plays a role in a variety of cellular functions, including cell proliferation, changes in cell shape, and motility and transport of intracellular organelles. It has been demonstrated that microtubules enriched in TUBB3 are considerably more dynamic than those composed of other β-tubulin isotypes [42]. Moreover, recent data show that mutations in human *TUBB3* can lead to diverse neurological syndromes, likely caused by defects in neuronal migration and differentiation, impairment of axonal guidance, disturbances in microtubule dynamics and interactions with kinesin and other microtubule-interacting proteins [43, 44]. In this context, it is important to note that earlier reports have found similarities between microtubule organization in neuronal axons and SC processes [45]. In addition, both cell types share a susceptibility to toxins affecting the cytoskeleton [45]. In this regard, we note that aberrant expression of *Tubb3* in a variety of tumors (including ovarian, breast and lung cancers) results in increased resistance to antimitotic agents, such as paclitaxel, that target the tubulin/microtubule system [11, 46]. Interestingly, recent studies have shown that *Tubb3* is also an inherent component of mitochondrial membranes, where it interacts with a voltage-dependent anion channel. Although this mitochondrial tubulin represents only some 2% of the total cellular tubulin, it may be crucial for specific processes, such as induction of apoptosis and adaptation to oxidative stress or glucose deprivation [47, 48].

The finding that *Tubb3* expression in SCs is controlled by androgens may also be of interest for other fields: *Tubb* genes have been shown to be androgen regulated in terminally differentiated neurons, the only other cell type that normally expresses TUBB3 [5]. Androgens have complex effects on the development of the male nervous system, the activation of specific neuronal circuits, and the responses of neurons to nerve injuries [49, 50]. Several of these effects are accompanied by changes in cytoskeletal gene expression. For instance, castration significantly reduced β-tubulin mRNA in motor neurons in the spinal nucleus of the bulbocavernosus (SNB), an effect prevented by androgen treatment [51]. Androgen-induced growth of the SNB motor neuron somata and dendrites is accompanied by marked changes in the expression of β-actin and β-tubulin [52]. Similarly, the androgen-induced increase in the rate of axonal regeneration after facial nerve injury occurs concomitantly with increased β-tubulin expression [53]. It remains to be determined which β-tubulin isoforms are involved in these effects. Finally, androgens induce upregulation of the ubiquitous βII-tubulin and the neuron-specific βIII-tubulin in AR-expressing human SH-SY5Y neuroblastoma cells [54]. This increase was abolished by cotreatment with antiandrogens, suggesting that androgens regulate tubulins in neural cells through direct activation of the AR [54].

Taken together, our data indicate that *Tubb3* is a target of androgen action in SCs from the initiation of meiosis to adult spermatogenesis. The significant changes in both mRNA and protein levels detected in vivo and in vitro and the identification of a cluster of AREs in the *Tubb3* gene strongly suggest that androgens modulate microtubular composition and structure through a direct action on *Tubb3*. *Tubb3* is a particularly compelling target of androgen action given that it is exclusively expressed in SCs, which is the cell type in which AR mediates many of its actions on spermatogenesis. Thus, it is tempting to speculate that androgens exert at least part of their effects on spermatogenesis through upregulation of TUBB3 levels in SCs, thereby inducing functional changes in the SC cytoskeleton, which in turn are likely to contribute to the tubular restructuring that accompanies the onset and progression of spermatogenesis. The development of a SC-selective knockout of this β-tubulin isotype will address this important issue in the future.

ACKNOWLEDGMENTS

REFERENCES

1. Sharpe RM. Regulation of spermatogenesis. In: Knobil E, Neill JD (eds.), The Physiology of Reproduction, 2nd ed. New York: Raven Press; 1994:1363–1434.
2. De Gendt K, Swinnen JV, Saunders PT, Schoonjans L, Dewerchin M, Devos A, Tan K, Atanassova N, Claessens F, Lecureuil C, Heyns W, Carmeliet P, et al. A Sertoli cell-selective knockout of the androgen receptor causes spermatogenic arrest in meiosis. Proc Natl Acad Sci U S A 2004; 101:1327–1332.
3. Welsh M, Saunders PT, Atanassova N, Sharpe RM, Smith LB. Androgen action via testicular peritubular myoid cells is essential for male fertility. FASEB J 2009; 23:4218–4230.
4. Denolet E, De Gendt K, Allemeersch J, Engelen K, Marchal K, Van Hummelen P, Tan KA, Sharpe RM, Saunders PT, Swinnen JV, Verhoeven G. The effect of a sertoli cell-selective knockout of the androgen receptor on testicular gene expression in prepubertal mice. Mol Endocrinol 2006; 20:321–334.
5. Lee MK, Rebhun LI, Frankfurter A. Posttranslational modification of class III beta-tubulin. Proc Natl Acad Sci U S A 1990; 87:7195–7199.
6. Lewis SA, Cowan NJ. Complex regulation and functional versatility of mammalian alpha- and beta-tubulin isotypes during the differentiation of testis and muscle cells. J Cell Biol 1988; 106:2023–2033.
7. Liu L, Geisert EE, Frankfurter A, Spano AJ, Jiang CX, Yue J, Dragatsis I, Goldowitz D. A transgenic mouse class-III beta tubulin reporter using yellow fluorescent protein. Genesis 2007; 45:560–569.

8. Dennis K, Uittenbogaard M, Chiaramello A, Moody SA. Cloning and characterization of the 5′-flanking region of the rat neuron-specific Class III beta-tubulin gene. Gene 2002; 294:269–277.

9. Sullivan KF, Cleveland DW. Identification of conserved isotype-defining variable region sequences for four vertebrate beta tubulin polypeptide classes. Proc Natl Acad Sci U S A 1986; 83:4327–4331.

10. Vogl AW, Pfeiffer DC, Redenbach DM, Grove BD. Sertoli cell cytoskeleton. In: Russell LD, Griswold MD (eds.), The Sertoli Cell, 1st ed. Clearwater: Cache River Press; 1993:39–86.

11. Gan PP, Pasquier E, Kavallaris M. Class III beta-tubulin mediates sensitivity to chemotherapeutic drugs in non small cell lung cancer. Cancer Res 2007; 67:9356–9363.

12. O'Shaughnessy PJ, Abel M, Charlton HM, Hu B, Johnston H, Baker PJ. Altered expression of genes involved in regulation of vitamin A metabolism, solute transportation, and cytoskeletal function in the androgen-insensitive tfm mouse testis. Endocrinology 2007; 148:2914–2924.

13. Verhoeven G, Cailleau J. Testicular peritubular cells secrete a protein under androgen control that inhibits induction of aromatase activity in Sertoli cells. Endocrinology 1988; 123:2100–2110.

14. De Gendt K, McKinnell C, Willems A, Saunders PT, Sharpe RM, Atanassova N, Swinnen JV, Verhoeven G. Organotypic cultures of prepubertal mouse testes: a method to study androgen action in Sertoli cells while preserving their natural environment. Biol Reprod 2009; 81:1083–1092.

15. Johnston H, Baker PJ, Abel M, Charlton HM, Jackson G, Fleming L, Kumar TR, O'Shaughnessy PJ. Regulation of Sertoli cell number and activity by follicle-stimulating hormone and androgen during postnatal development in the mouse. Endocrinology 2004; 145:318–329.

16. Banerjee A, Roach MC, Trcka P, Luduena RF. Preparation of a monoclonal antibody specific for the class IV isotype of beta-tubulin. Purification and assembly of alpha beta II, alpha beta III, and alpha beta IV tubulin dimers from bovine brain. J Biol Chem 1992; 267:5625–5630.

17. Banerjee A, Roach MC, Wall KA, Lopata MA, Cleveland DW, Luduena RF. A monoclonal antibody against the type II isotype of beta-tubulin. Preparation of isotypically altered tubulin. J Biol Chem 1988; 263:3029–3034.

18. Banerjee A, Roach MC, Trcka P, Luduena RF. Increased microtubule assembly in bovine brain tubulin lacking the type III isotype of beta-tubulin. J Biol Chem 1990; 265:1794–1799.

19. Lewis SA, Lee MG, Cowan NJ. Five mouse tubulin isotypes and their regulated expression during development. J Cell Biol 1985; 101:852–861.

20. De Gendt K, Atanassova N, Tan KA, de Franca LR, Parreira GG, McKinnell C, Sharpe RM, Saunders PT, Mason JI, Hartung S, Ivell R, Denolet E, et al. Development and function of the adult generation of Leydig cells in mice with Sertoli cell-selective or total ablation of the androgen receptor. Endocrinology 2005; 146:4117–4126.

21. Legler J, van den Brink CE, Brouwer A, Murk AJ, van der Saag PT, Vethaak AD, van der Burg B. Development of a stably transfected estrogen receptor-mediated luciferase reporter gene assay in the human T47D breast cancer cell line. Toxicol Sci 1999; 48:55–66.

22. Denayer S, Helsen C, Thorrez L, Haelens A, Claessens F. The rules of DNA recognition by the androgen receptor. Mol Endocrinol 2010; 24:898–913.

23. Walther N, Jansen M, Ergun S, Kascheike B, Ivell R. Sertoli cell lines established from H-2Kb-tsA58 transgenic mice differentially regulate the expression of cell-specific genes. Exp Cell Res 1996; 225:411–421.

24. Haelens A, Tanner T, Denayer S, Callewaert L, Claessens F. The hinge region regulates DNA binding, nuclear translocation, and transactivation of the androgen receptor. Cancer Res 2007; 67:4514–4523.

25. Verrijdt G, Haelens A, Schoenmakers E, Rombauts W, Claessens F. Comparative analysis of the influence of the high-mobility group box 1 protein on DNA binding and transcriptional activation by the androgen, glucocorticoid, progesterone and mineralocorticoid receptors. Biochem J 2002; 361:97–103.

26. Schoenmakers E, Alen P, Verrijdt G, Peeters B, Verhoeven G, Rombauts W, Claessens F. Differential DNA binding by the androgen and glucocorticoid receptors involves the second Zn-finger and a C-terminal extension of the DNA-binding domains. Biochem J 1999; 341(pt 3):515–521.

27. Schauwaers K, De Gendt K, Saunders PT, Atanassova N, Haelens A, Callewaert L, Moehren U, Swinnen JV, Verhoeven G, Verrijdt G, Claessens F. Loss of androgen receptor binding to selective androgen response elements causes a reproductive phenotype in a knockin mouse model. Proc Natl Acad Sci U S A 2007; 104:4961–4966.

28. Turatsinze JV, Thomas-Chollier M, Defrance M, van HJ. Using RSAT to scan genome sequences for transcription factor binding sites and cis-regulatory modules. Nat Protoc 2008; 3:1578–1588.

29. Claessens F, Celis L, Peeters B, Heyns W, Verhoeven G, Rombauts W. Functional characterization of an androgen response element in the first intron of the C3(1) gene of prostatic binding protein. Biochem Biophys Res Commun 1989; 164:833–840.

30. Heemers H, Verrijdt G, Organe S, Claessens F, Heyns W, Verhoeven G, Swinnen JV. Identification of an androgen response element in intron 8 of the sterol regulatory element-binding protein cleavage-activating protein gene allowing direct regulation by the androgen receptor. J Biol Chem 2004; 279:30880–30887.

31. Lund SD, Gallagher PM, Wang B, Porter SC, Ganschow RE. Androgen responsiveness of the murine beta-glucuronidase gene is associated with nuclease hypersensitivity, protein binding, and haplotype-specific sequence diversity within intron 9. Mol Cell Biol 1991; 11:5426–5434.

32. Tapanainen JS, Aittomaki K, Min J, Vaskivuo T, Huhtaniemi IT. Men homozygous for an inactivating mutation of the follicle-stimulating hormone (FSH) receptor gene present variable suppression of spermatogenesis and fertility. Nat Genet 1997; 15:205–206.

33. Singh J, O'Neill C, Handelsman DJ. Induction of spermatogenesis by androgens in gonadotropin-deficient (hpg) mice. Endocrinology 1995; 136:5311–5321.

34. Kumar TR, Wang Y, Lu N, Matzuk MM. Follicle stimulating hormone is required for ovarian follicle maturation but not male fertility. Nat Genet 1997; 15:201–204.

35. Dierich A, Sairam MR, Monaco L, Fimia GM, Gansmuller A, LeMeur M, Sassone-Corsi P. Impairing follicle-stimulating hormone (FSH) signaling in vivo: targeted disruption of the FSH receptor leads to aberrant gametogenesis and hormonal imbalance. Proc Natl Acad Sci U S A 1998; 95:13612–13617.

36. Heemers H, Maes B, Foufelle F, Heyns W, Verhoeven G, Swinnen JV. Androgens stimulate lipogenic gene expression in prostate cancer cells by activation of the sterol regulatory element-binding protein cleavage activating protein/sterol regulatory element-binding protein pathway. Mol Endocrinol 2001; 15:1817–1828.

37. Bhardwaj A, Rao MK, Kaur R, Buttigieg MR, Wilkinson MF. GATA factors and androgen receptor collaborate to transcriptionally activate the Rhox5 homeobox gene in Sertoli cells. Mol Cell Biol 2008; 28:2138–2153.

38. Barbulescu K, Geserick C, Schuttke I, Schleuning WD, Haendler B. New androgen response elements in the murine pem promoter mediate selective transactivation. Mol Endocrinol 2001; 15:1803–1816.

39. Schoenherr CJ, Paquette AJ, Anderson DJ. Identification of potential target genes for the neuron-restrictive silencer factor. Proc Natl Acad Sci U S A 1996; 93:9881–9886.

40. Bruhat A, Dreau D, Drake ME, Tourmente S, Chapel S, Couderc JL, Dastugue B. Intronic and 5′ flanking sequences of the Drosophila beta 3 tubulin gene are essential to confer ecdysone responsiveness. Mol Cell Endocrinol 1993; 94:61–71.

41. Willems A, De Gendt K, Allemeersch J, Smith LB, Welsh M, Swinnen JV, Verhoeven G. Early effects of Sertoli cell-selective androgen receptor ablation on testicular gene expression. Int J Androl 2010; 33:507–517.

42. Panda D, Miller HP, Banerjee A, Luduena RF, Wilson L. Microtubule dynamics in vitro are regulated by the tubulin isotype composition. Proc Natl Acad Sci U S A 1994; 91:11358–11362.

43. Tischfield MA, Baris HN, Wu C, Rudolph G, Van ML, He W, Chan WM, Andrews C, Demer JL, Robertson RL, Mackey DA, Ruddle JB, et al. Human TUBB3 mutations perturb microtubule dynamics, kinesin interactions, and axon guidance. Cell 2010; 140:74–87.

44. Poirier K, Saillour Y, Bahi-Buisson N, Jaglin XH, Fallet-Bianco C, Nabbout R, Castelnau-Ptakhine L, Roubertie A, Attie-Bitach T, Desguerre I, Genevieve D, Barnerias C, et al. Mutations in the neuronal {beta}-tubulin subunit TUBB3 result in malformation of cortical development and neuronal migration defects. Hum Mol Genet 2010; 19:4462–4473.

45. Neely MD, Boekelheide K. Sertoli cell processes have axoplasmic features: an ordered microtubule distribution and an abundant high molecular weight microtubule-associated protein (cytoplasmic dynein). J Cell Biol 1988; 107:1767–1776.

46. Kavallaris M, Burkhart CA, Horwitz SB. Antisense oligonucleotides to class III beta-tubulin sensitize drug-resistant cells to Taxol. Br J Cancer 1999; 80:1020–1025.

47. Carre M, Andre N, Carles G, Borghi H, Brichese L, Briand C, Braguer D. Tubulin is an inherent component of mitochondrial membranes that interacts with the voltage-dependent anion channel. J Biol Chem 2002; 277:33664–33669.

48. Cicchillitti L, Penci R, Di MM, Filippetti F, Rotilio D, Donati MB,

Scambia G, Ferlini C. Proteomic characterization of cytoskeletal and mitochondrial class III beta-tubulin. Mol Cancer Ther 2008; 7:2070–2079.

49. Morris JA, Jordan CL, Breedlove SM. Sexual differentiation of the vertebrate nervous system. Nat Neurosci 2004; 7:1034–1039.

50. Raskin K, De Gendt K, Duittoz A, Liere P, Verhoeven G, Tronche F, Mhaouty-Kodja S. Conditional inactivation of androgen receptor gene in the nervous system: effects on male behavioral and neuroendocrine responses. J Neurosci 2009; 29:4461–4470.

51. Matsumoto A, Arai Y, Hyodo S. Androgenic regulation of expression of beta-tubulin messenger ribonucleic acid in motoneurons of the spinal nucleus of the bulbocavernosus. J Neuroendocrinol 1993; 5:357–363.

52. Matsumoto A, Arai Y, Urano A, Hyodo S. Androgen regulates gene expression of cytoskeletal proteins in adult rat motoneurons. Horm Behav 1994; 28:357–366.

53. Jones KJ, Oblinger MM. Androgenic regulation of tubulin gene expression in axotomized hamster facial motoneurons. J Neurosci 1994; 14:3620–3627.

54. Butler R, Leigh PN, Gallo JM. Androgen-induced up-regulation of tubulin isoforms in neuroblastoma cells. J Neurochem 2001; 78:854–861.